

Growth and Characterization of $\text{InAs}_{1-x}\text{Sb}_x$ with Different Sb Compositions on GaAs Substrates *

SUN Qing-Ling(孙庆灵)^{1,2}, WANG Lu(王禄)^{1,2,3**}, WANG Wen-Qi(王文奇)^{1,2}, SUN Ling(孙令)^{1,2},
LI Mei-Cheng(李美成)³, WANG Wen-Xin(王文新)^{1,2}, JIA Hai-Qiang(贾海强)^{1,2},
ZHOU Jun-Ming(周均铭)^{1,2}, CHEN Hong(陈弘)^{1,2}

¹Key Laboratory for Renewable Energy, Institute of Physics, Chinese Academy of Sciences, Beijing 100190

²Beijing Key Laboratory for New Energy Materials and Devices, Beijing National Laboratory for Condensed Matter Physics, and Institute of Physics, Chinese Academy of Sciences, Beijing 100190

³State Key Laboratory of Alternate Electrical Power System with Renewable Energy Sources, School of Renewable Energy, North China Electric Power University, Beijing 102206

(Received 25 May 2015)

InAs_{1-x}Sb_x with different compositions is grown by molecular beam epitaxy on (100)-oriented semi-insulating GaAs substrates. The increase of Sb content in the epilayer results in the deterioration of crystal quality and surface morphology. Hall measurements show that the carrier concentration increases with the composition of Sb. The electron mobility decreases initially, when Sb composition exceeds a certain value, and the mobility increases slightly. In this work, we emphasize the comparison of crystal quality, surface morphology and electrical properties of epilayers with different Sb compositions.

PACS: 68.37.-d, 61.05.-a, 81.15.-z, 81.05.Ea

DOI: 10.1088/0256-307X/32/10/106801

InAsSb is an ideal material for the preparation of infrared detectors. It has the narrowest band gap in the family of III-V compounds. In terms of infrared detection, the detection wavelength of InAsSb-based infrared detectors covers mid-wave infrared (MWIR) and long-wave infrared (LWIR). There are many reports on InAsSb-based infrared detectors, including photoconductive detectors,^[1] photovoltaic detectors,^[2,3] nBn detectors.^[4,5] A high-quality InAsSb epitaxial layer is the prerequisite for the fabrication of devices.

InAsSb epitaxial layers have been fabricated on GaAs,^[6,7] InAs,^[8] InP^[9] and GaSb^[10,11] substrates. For the material system with large mismatch, the high-quality epitaxial layer is not easily obtained. The use of intermediate buffer^[12] or nucleation layer^[13] is beneficial to the improvement of the epitaxial quality. InAsSb ternary on GaAs has a lattice mismatch between 7.2% and 14.5%, depending on the content of Sb. The use of InAs nucleation layer may be a good way for the acquisition of high-quality InAsSb. Moreover, the peak response of InAsSb-based infrared detection devices includes middle wavelengths and long wavelengths, and the wavelength depends on Sb composition. Thus it is important to characterize the properties of InAsSb layers with different compositions. However, the accurate control of composition is not easy for the alloy with double V-group elements. In this work, InAsSb alloys with different composi-

tions are grown on GaAs substrates by changing Sb flux. The influence of Sb compositions on crystal quality and electrical property was analyzed. Although the growth of InAsSb epilayer has been reported by others, few have focused on the comparison of different InAsSb epilayers. Therefore, crystal structure, morphology and electrical property of different Sb composition InAsSb epilayers are investigated systematically in our work.

The epitaxial growth was performed in a VG Semicon V80 molecular beam epitaxy (MBE) system equipped with a valved arsenic cracker cell and an effusion antimony cell. Beam fluxes were measured by an ion gauge positioned in the growth chamber. The growth of the sample includes two steps. First, a 20 nm InAs nucleation layer was deposited on a GaAs substrate at 405°C, followed by a 1.5 μm $\text{InAs}_{1-x}\text{Sb}_x$ ($x = 0\%$, 5%, 8.8% and 11%) layer at 450°C. The V-III flux ratio of As and In was fixed at 10 for all the samples, and different Sb compositions were achieved by varying the Sb beam flux. The growth rate depending on indium beam flux was 6000 Å/h.

The Hall-effect measurement was performed at room temperature (300 K) and low temperature (77 K) on the samples to determine the electrical property. The morphology of the epitaxial layer was studied by using scanning electron microscope (SEM) and atomic force microscope (AFM). Composition and crystalline quality of the epilayer were characterized

*Supported by the Aeronautical Science Foundation of China under Grant No 20132435, the National High-Techonology Research and Development Program of China under Grant No 2013AA031903, the National Natural Science Foundation of China under Grant Nos 61106013 and 61275107, and the China Postdoctoral Science Foundation under Grant No 2014M560936.

**Corresponding author. Email: lwang@iphy.ac.cn

© 2015 Chinese Physical Society and IOP Publishing Ltd

by double-crystal x-ray diffraction (XRD), by using a Cu $K\alpha$ source.

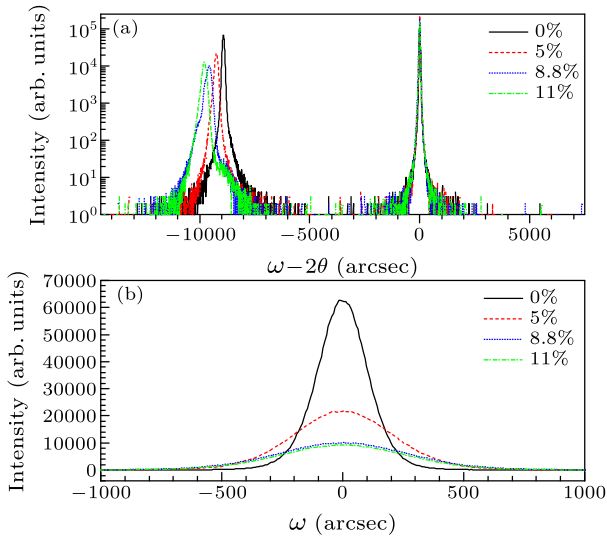


Fig. 1. X-ray diffraction patterns: (a) $\omega-2\theta$ curves of $\text{InAs}_{1-x}\text{Sb}_x$, (b) x-ray rocking curves of $\text{InAs}_{1-x}\text{Sb}_x$.

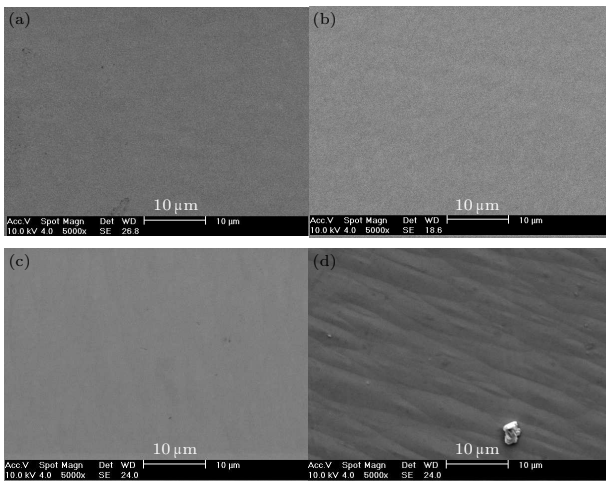


Fig. 2. Scanning electron micrograph of the epilayers: (a) $x = 0$, (b) $x = 5\%$, (c) $x = 8.8\%$, and (d) $x = 11\%$.

X-ray diffraction in (004) and (115) orientations was measured to assess the crystal quality and to determine the composition of the epilayer. Figure 1(a) shows the $\omega-2\theta$ curves of the epilayers. For each sample, there is only a narrow peak of epilayer in addition to the peak of the substrate. No phase separation as reported by others^[14] was observed in our samples. The accurate value of full width at half maximum (FWHM) could be obtained from the x-ray rocking curves. The comparison of x-ray rocking curves in Fig. 1(b) indicates that the increase of Sb results in broader x-ray diffraction peaks ($\text{FWHM} > 600$ arcsec), while the InAs epilayer has a narrow FWHM (236 arcsec). The FWHM reduces much compared with samples by using other nucleation layers.^[15] From the x-ray diffraction measurements we could conclude that the high Sb composi-

tion in the epilayer leads to worse crystal quality, and this can be attributed to lattice mismatch. The lattice constant of InSb is larger than InAs, the increase of Sb composition results in the deterioration of crystal quality. The strain relaxations acquired by x-ray diffraction from planes of symmetry and asymmetry are 99.85%, 99.26% and 99.63% for the Sb compositions of 5%, 8.8% and 11%, respectively. This indicates that the samples have nearly full relaxation.

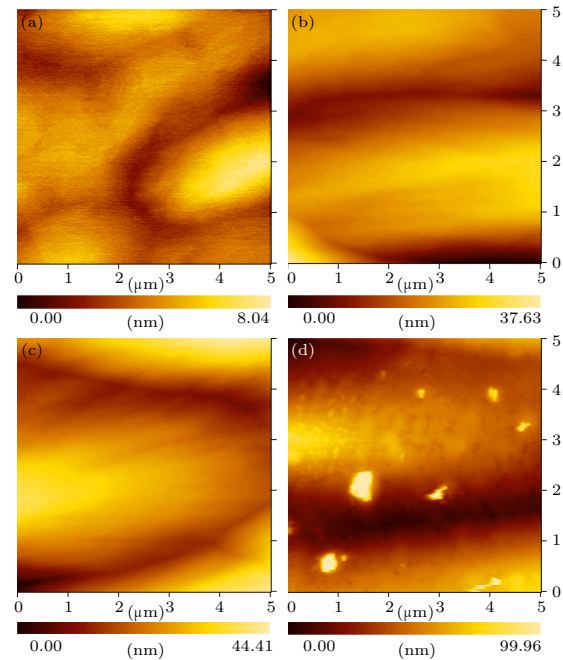


Fig. 3. AFM images of $\text{InAs}_{1-x}\text{Sb}_x$ epilayers: (a) $x = 0$, (b) $x = 5\%$, (c) $x = 8.8\%$, and (d) $x = 11\%$.

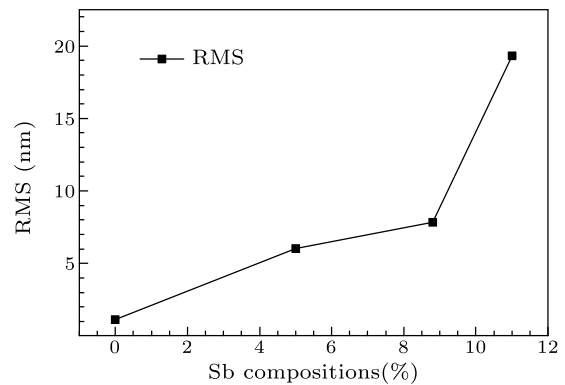


Fig. 4. Dependence of rms roughness on Sb compositions.

AFM and SEM measurements were performed to study the surface morphology. From the SEM images (Fig. 2) we can see that samples with a low Sb composition have a flat surface with no obvious defects. With the increase of Sb compositions, the surface becomes uneven, and some distinct defects appear on the surface. AFM can characterize the surface roughness quantitatively with high accuracy. The rms roughness was measured over a $5 \times 5 \mu\text{m}^2$ area for all sam-

ples. The surface roughness of InAs is around 1.14 nm (Fig. 3(a)). Due to the formation of defects on the surface, when Sb composition comes to 11%, the rms roughness of InAsSb increases up to 19.3 nm. The measured dependence of rms roughness on Sb compositions is shown in Fig. 4. From the results of AFM and SEM, we can see that the sample with a high Sb composition has a very uneven surface (Fig. 3(d)), and some surface defects can be seen clearly.

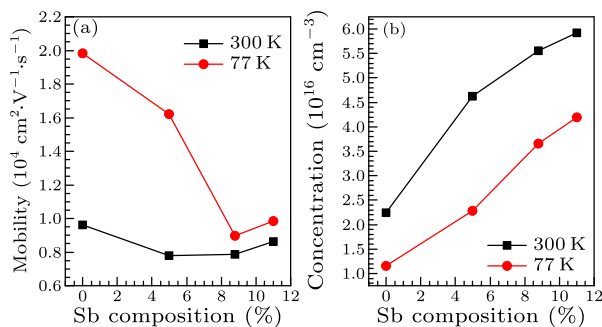


Fig. 5. Measured composition dependences of (a) Hall mobility and (b) concentration.

The formation of the observed surface morphology can be explained as follows. In the heteroepitaxial growth, the lattice relaxation caused by lattice mismatch has a great influence on surface morphology^[16,17] and properties.^[18] According to the model of Matthews *et al.*,^[19] for the epitaxial growth with lattice mismatch, there exists a critical thickness above which misfit dislocations would appear to reduce strain energy. For the growth of InAsSb on the GaAs substrate with the InAs nucleation layer, the process of growth includes two lattice relaxation processes. Firstly, the InAs film has a 7.2% lattice mismatch with the GaAs substrate, the epilayer is strained at the beginning, and the strain is relieved beyond the critical thickness through the formation of dislocations. Due to the large lattice mismatch, the InAs nucleation layer contains a large number of dislocations. Secondly, for the InAsSb film on the InAs nucleation layer, the InAsSb epilayer is strained at the beginning, and the strain is relieved beyond the critical thickness. Due to the fact that the InAs nucleation layers were grown under the same condition, the morphologies of the samples resulted from different Sb compositions. For the sample with Sb composition of 11%, the InAsSb film has a lattice mismatch of 0.76% with the InAs layer, a large number of dislocations were formed in the process of strain relaxation. Thus the rugged surface is formed by large lattice mismatch and strain relaxation. The defect density depends on lattice mismatch. Therefore, the sample with high Sb content (11%) has a distinctively rough surface.

Room temperature (300 K) and low temperature (77 K) Hall-effect measurements were carried out on all the samples by using Van der Pauw's method. The

electron mobility and concentration values of the samples are listed in Table 1. The presence of defects in the lattice-mismatched system has a great influence on the results of Hall-effect measurements. Figure 5 shows the variation of mobility and concentration with Sb compositions. The mobility decreases with the increase of Sb compositions initially. When Sb composition reaches 11%, the mobility has a slight increase. The decrease of mobility can be attributed to the large lattice mismatch caused by high Sb composition. Due to the fact that the mobility of InSb is higher than InAs, the mobility of InAsSb increases when Sb composition is high enough. Thus the mobility increases when Sb composition is 11%. The defects caused by lattice mismatch act as donors providing electrons, as a result, the concentration increases with the composition of Sb. The electrical property is in good agreement with the results of XRD, SEM and AFM. The samples with good crystal quality and flat surface have high electron mobility and low concentration. The Sb composition in the InAsSb-based nBn type detector is 9%. In our experiments, the sample with Sb composition of 8.8% is an ideal material used for the InAsSb-based nBn type detector.

Table 1. Results of Hall-effect measurements.

Composition x	Mobility (cm^2/Vs)		Concentration (cm^{-3})	
	300 K	77 K	300 K	77 K
0%	9636	19823	2.24×10^{16}	1.16×10^{16}
5%	7776	16205	4.62×10^{16}	2.28×10^{16}
8.8%	7853	8968	5.55×10^{16}	3.66×10^{16}
11%	8626	9855	5.92×10^{16}	4.19×10^{16}

Infrared detection is one of the important applications of InAsSb. Since the nBn type infrared detector was proposed by Maimon *et al.*,^[20] the InAsSb-based nBn infrared detector has attracted great interests. Although the large lattice mismatch exists between InAsSb and the GaAs substrate, good crystal quality can be acquired by using a nucleation layer. Furthermore, the GaAs substrate has the advantages of low cost and mature processing technology. Also, the performance of InAsSb-based bariodes on the GaAs substrate is comparable with equivalent structures grown on GaSb,^[21,22] this may be attributed to the special energy band structure. Thus the study of InAsSb grown on the GaAs substrate is important for the preparation of InAsSb-based devices.

In summary, InAsSb epilayers with different Sb compositions have been grown on semi-insulating GaAs substrates with an InAs nucleation layer. The InAs epilayer has a good crystal quality and flat surface without any surface defects. The crystal quality of InAsSb deteriorates with the increase of Sb composition, and surface defects appear on the epilayer with high Sb composition (11%). It is evident that the electrical property is dependent on the crystal quality and surface roughness. The influence of Sb compositions

on crystal quality, surface morphology and electrical properties is studied systematically.

References

- [1] Kim J D, Wu D, Wojkowski J, Piotrowski J, Xu J and Razeghi M 1996 *Appl. Phys. Lett.* **68** 99
- [2] Rakovska A, Berger V, Marcadet X, Vinter B, Glastre G, Oksenhendler T and Kaplan D 2000 *Appl. Phys. Lett.* **77** 397
- [3] Kim J D, Kim S, Wu D, Wojkowski J, Xu J, Piotrowski J, Bigan E and Razeghi M 1995 *Appl. Phys. Lett.* **67** 2645
- [4] Khoshakhlagh A, Myers S, Plis E, Kutty M N, Klein B, Gautam N, Kim H, Smith E P G, Rhiger D, Johnson S M and Krishna S 2010 *Proc. SPIE* **7660** 76602Z-1
- [5] Myers S A, Khoshakhlagh A, Mailfert J, Wanninkhof P, Plis E, Kutty M N, Kim H S, Gautam, N, Klein B, Smith E P G and Krishna S 2010 *Proc. SPIE* **7808** 780805
- [6] Yen M Y, People R and Wecht K W 1988 *J. Appl. Phys.* **64** 952
- [7] Besikci C, Choi Y H, Labeyrie G, Bigan E, Razeghi M, Cohen J B, Carsello J and Dravid V P 1994 *J. Appl. Phys.* **76** 5820
- [8] Cheung D T, Andrews A M, Gertner E R, Williams G M, Clarke J E, Pasko J G and Longo J T 1977 *Appl. Phys. Lett.* **30** 587
- [9] Tsukamoto S, Bhattacharya P, Chen Y C and Kim J H 1990 *J. Appl. Phys.* **67** 6819
- [10] Rakovska A, Berger V, Marcadet X, Vinter B, Bouzheouane K and Kaplan D 2000 *Semicond. Sci. Technol.* **15** 34
- [11] Marciniak M A, Hengehold R L, Yeo Y K and Turner G W 1998 *J. Appl. Phys.* **84** 480
- [12] Li L K, Hsu Y and Wang W I 1993 *J. Vac. Sci. Technol. B* **11** 872
- [13] Ballal A K, Salamanca-Riba L, Partin D L, Heremans J, Green L and Fuller B K 1993 *J. Electron. Mater.* **22** 383
- [14] Miyoshi H, Suzuki R, Amano H and Horikoshi Y 2002 *J. Cryst. Growth* **237** 1519
- [15] Gao H C, Wang W X, Jiang Z W, Liu L S, Zhou J M and Chen H 2007 *J. Cryst. Growth* **308** 406
- [16] Snyder C W, Orr B G, Kessler D and Sander L M 1991 *Phys. Rev. Lett.* **66** 3032
- [17] Belk J G, Pashley D W, McConville C F, Joyce B A and Jones T S 1998 *Surf. Sci.* **410** 82
- [18] Pan Z, Wang Y T, Li L H, Wang H, Wei Z, Zhou Z Q and Lin Y W 1999 *J. Appl. Phys.* **86** 5302
- [19] Matthews J W and Blakeslee A E 1974 *J. Cryst. Growth* **27** 118
- [20] Maimon S and Wicks G W 2006 *Appl. Phys. Lett.* **89** 151109
- [21] Weiss E, Klin O, Grossmann S, Snapi N, Lukomsky I, Aronov D, Yassen M, Berkowicz E, Glozman A, Klipstein P, Fraenkel A and Shtrichman I 2012 *J. Cryst. Growth* **339** 31
- [22] Craig A P, Marshall A R J, Tian Z B and Krishna S 2014 *Infrared Phys. Technol.* **67** 210